GAS FLOW SHEAR INTERFEROGRAMS AND SHADOW PATTERNS INFORMATIVITY COMPARATIVE ANALYSIS

S.I. INSHAKOV [1], A.G. PELMENEV [2], A.YU. RODIONOV [2], A.S. SHIRIN [2], V.N. SHEKHTMAN [2]

[1] State Research Center "The Central Aerohydrodynamic Institute" (TsAGI), 140180, Zhukovsky, Moscow reg., Russia
[2] Engineering & Physics Laboratory (EFL Ltd.), 195197, Saint-Petersburg, Russia.
Corresponding author: Tel.: +7 812 466 0688; Fax: +7 812 331 9284; E-mail: shekhtman@mail.rcom.ru

KEYWORDS:

Main subjects: Shear interferometric and shadow methods comparison

Fluid: any type of medium, flows, gas-dynamic, turbulence, turbulence spectrum, and shocks

Visualization method(s): Shear interferometry, Toepler shadow method

Other keywords: interference pattern processing, spatial spectrum, wave front, Fourier spectra, vibration resistance.

ABSTRACT: Shear interferometric and shadow methods can be applied for the small-scale gas flows structure study, including turbulence characteristics. Shear interference and shadow patterns are often used to visualize the gas flow at small shear values and with maximum possible fringe width. Nevertheless mentioned patterns intensity spatial modulation contains various information especially about the flow statistical characteristics. This paper analyzed differences between the information contained in shear interferograms and shadow patterns Mentioned difference is illustrated by modeling experimental data

INTRODUCTION. Shear interferometric and shadow methods (Toepler method) represent a gas flow structure visualization and thermodynamic parameters distribution investigation instrument. Shear interferogram and shadow pattern look often determined by gas-dynamic medium integral density distribution along the testing beam as a reference light beam interferometric system. At the same time in several cases reference light beam interferometric systems has informational advantage over shear interferometry and shadow methods in terms of the equal sensitivity to gas-dynamic medium different inhomogeneity scales. However reference light beam interferometric system testbed implementation is a extremely complicated technical problem due to their high vibration sensitivity especially in cases of large scale stands. Moreover high-speed gas flow inhomogeneity and test object dimensions often lead to multiple breaks and contrast loss of interference fringes. In this case, mentioned interference pattern disadvantages practically can not be removed or compensated due to unregulated reference light beam interferometric systems sensitivity. Shadow methods are widely used to transparent inhomogeneity study including gas-dynamic medium due to mentioned reference light beam interference systems disadvantages.

This paper submits comparative shadow method and shear interferometry capabilities demonstration in gasdynamic studies. These capabilities are illustrated not so much shadow and interferometry methods well-known mathematical description analysis as the calculation models and experimental data demonstration. This approach seems more rewarding during the preliminary experiment planning, for example in turbulent gas flows study.

Shadow systems most prevalent on the gas dynamic study stands because of vibration resistance and density distribution picture visual perception accessibility, especially the flow around models. obtained with shadow patterns gas-dynamic medium density distribution reconstruction yield shear interferometry on results accuracy and density inhomogeneity spatial resolution as shown below despite researchers great attention of shadow patterns quantitative interpretation [1, 2]. In addition, shear interferometric method has the distinct advantage allowing to change interferometric system sensitivity and thus get available for quantitative processing interference pattern type with large density gradients. This fact greatly expands measurements dynamic range from slightly density inhomogeneous gas-dynamic medium to shock of the flows. However, informational limitations should take into account using shear interferometry systems. They determine embodiment and measurement methods specifics to fill the missing information including gas-dynamic medium thermodynamic parameters.

At least three uncertainties («information loss types») should be taken into account in the shear interferogram wave-front shape reconstruction results, [3, 4, 5].

DIRECTION DEPENDENT SENSITIVITY. First information loss type related to the fact that it's impossible to predict wave front function behavior in the orthogonal shear vector direction by shear interferogram form. for example, cylindrical and parabolic wave fronts are impossible to distinguish on the lateral shear interferogram. Indeed, for these distortion types wavefront functions correspond:

$$\varphi_p(x,y) = A\cdot(x^2+y^2)/(2\cdot R); \quad \varphi_z(x,y) = A\cdot x^2/(2\cdot R),$$

and corresponding to the shear interferograms difference functions will have the same form:

$$\psi_x(x,y) = \varphi(x,y) - \varphi(x+s,y) = A\frac{x \cdot s}{R},$$

here A – normalizing factor, s - shear value.

Instrument sensitivity anisotropy to the knife direction appears less in the shadow method. Shear and shadow method phase distortions registration systems numerical modeling done to illustrate this feature. Harmonic phase grating distortion model type was used as the phase distortion:

$$\varphi(x,y) = \sin\left[2\pi\left(\frac{x}{T_x} + \frac{y}{T_y}\right)\right] \quad (1),$$

where T_x, T_y – harmonic modulation period along the transverse coordinates.

Shadow instrument optical scheme is shown in Fig. 1, and shear interferometer - in Fig. 2.

Wave takes place at the entrance of both measurement systems represented in the calculation of the complex amplitude $A(x,y) = A_o\ exp(ik\varphi(x,y))$. Telescopic system with magnification equal to one accepted for systems Fig. 1 and Fig. 2 giving entrance pupil of diameter D image in the detection plane. In this intensity and phase uniform light wave φ(x,y) expected in the entrance pupil plane spaced a distance of $4 \cdot f$ from the image plane.

Measuring systems radiation propagation calculation made by solving the parabolic wave equation in paraxial approximation. Thus the light field complex amplitude distribution $A_1(x,y)$ determined on the shadow instrument and shearing interferometer exit pupil simulating a real shadow or shear pattern.

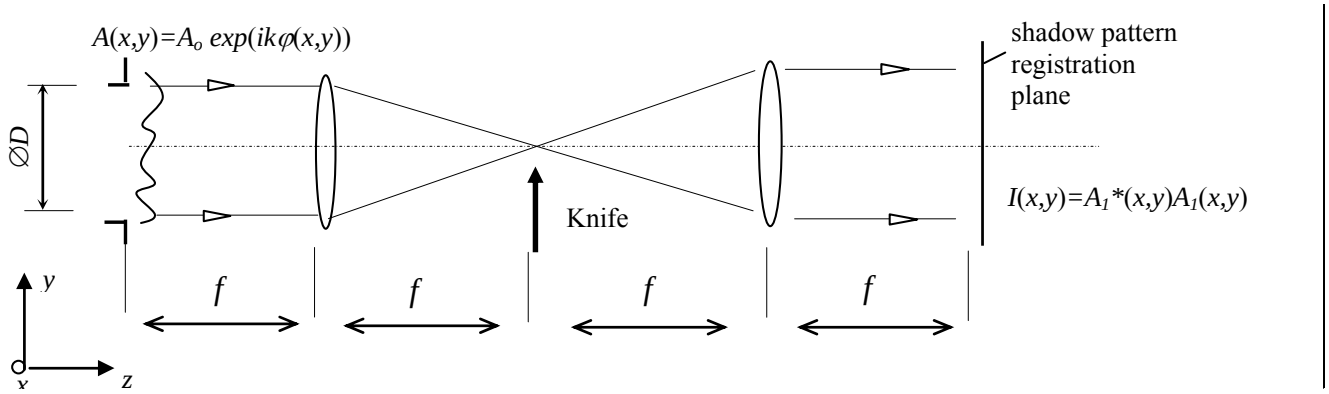

Fig.1. Shadow instrument scheme

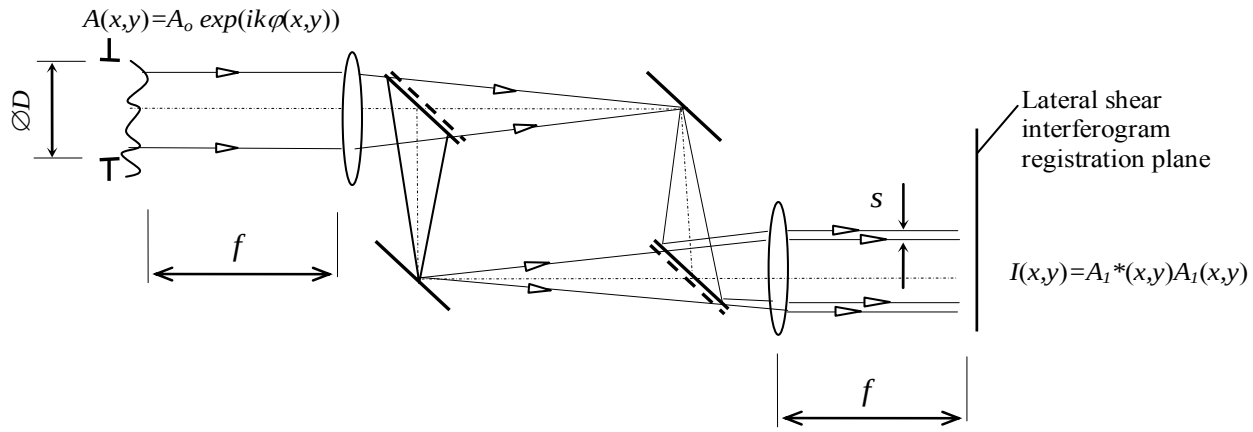

Fig.2. Lateral shear interferometer scheme

Fig. 3 shows the shear interferograms and shadow patterns for the two harmonic distortion orientations. Distortions entered in the calculation program description and other information about the model experiment are given below the figure. Informativity both shear interferometric and shadow systems depends strongly on the relative orientation of the probing the medium wave phase modulation gradient vector and shear direction or shadow instrument knife edge illustrated modulated wavefront intensity distribution shown on Fig. 3. Sensitivity anisotropy may result to complete signal loss, for example, with mutually perpendicular phase modulation gradient direction or mutually parallel image shear and knife edge.

Recording with two noncollinear shear vectors and knife directions has to carry out to this information loss problem. For example, two mutually orthogonal shear vectors s_x and s_y interferogram commonly used in the case of lateral shear interferometer.

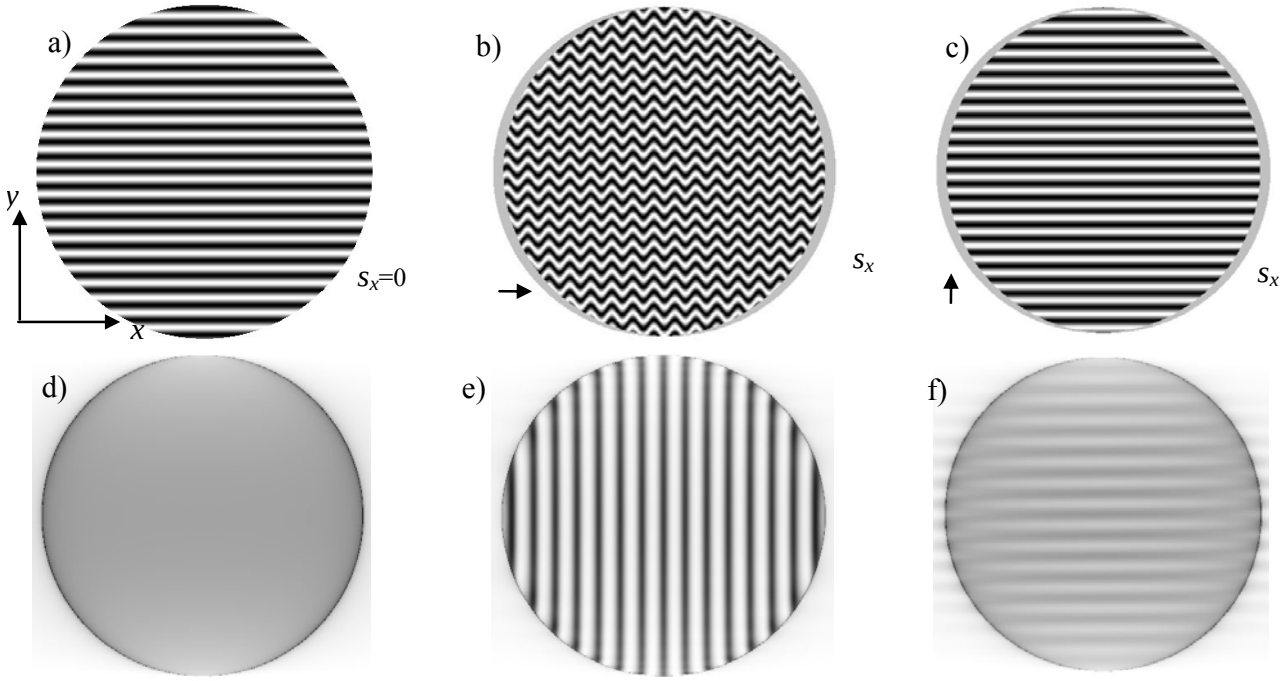

Fig.3. Lateral shear interferograms (a, b, c) and shadow patterns (d, e, f) with different orientation harmonic inhomogeneities (arrow on b and c):

b) and e): $\varphi(x,y) = \sin\left[2\pi\left(\frac{x}{T_o}\right)\right]$; c) and f): $\varphi(x,y) = \sin\left[2\pi\left(\frac{x}{100\cdot T_o} + \frac{y}{T_o}\right)\right]$;

spatial period – T_o=D/20; interferogram image shear b) and c) – $s_x = D/40$;

a) – lateral shear interferometer configuration image;

b) – shear interferogram maximum signal in case of $s_x = 0{,}5\cdot T_o$;

c) –signal absence for orthogonal directions of phase modulation gradient and shear;

d) – exit pupil plane radiation intensity distribution in the absence of knife;

e) – knife edge is perpendicular to phase modulation gradient (parallel to shadow pattern intensity modulation stripes);

f) – knife edge is parallel to phase modulation gradient, additional harmonic entered to indicate parallel to intensity stripes knife edge position.

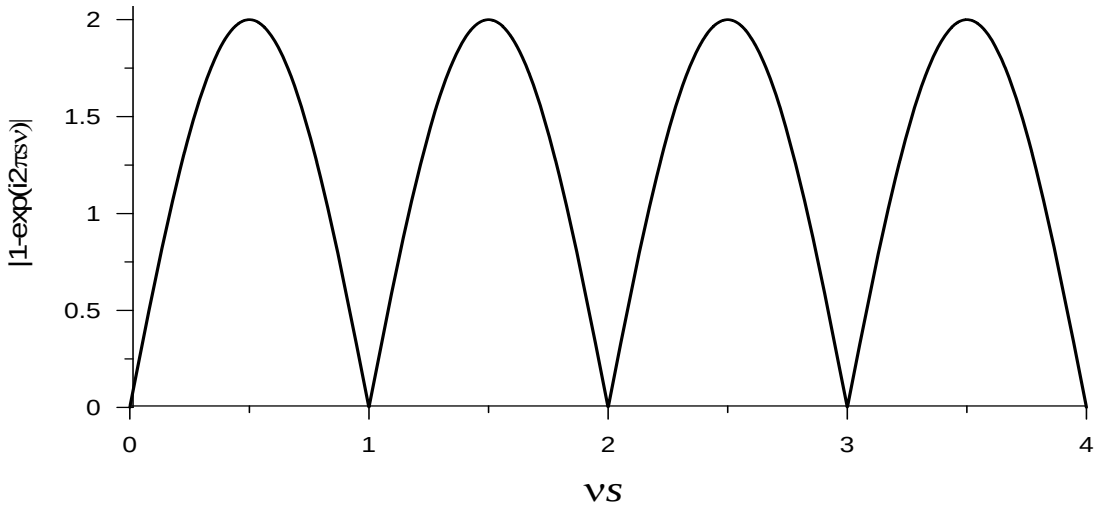

Fig.4. Lateral shear interferometer transfer function modulus graph.

SPATIAL FREQUENCIES SELECTIVE SENSITIVITY. Second data loss type associated with shear interferometers selective sensitivity to a wavefront deformation spatial frequencies, including complete sensitivity loss at certain frequencies [5, 6].So in the case of lateral shear difference function Fourier spectra ψ(x) = φ(x) – φ(x-s) and wavefront function φ(x) (one dimension case is sufficient) are related to each other:

$$H(\nu) = \Phi(\nu) \cdot \left[1 - \exp(-i2\pi s\nu)\right]$$
$$H(\nu) = F\left[\psi(x)\right], \quad \Phi(\nu) = F\left[\varphi(x)\right]. \qquad (2)$$

where F – Fourier transform operator.

Function $\Omega(\nu) = \left[1 - \exp(-i2\pi s\nu)\right]$ represents the lateral shear interferogram transfer function. Function modulus graph Ω(ν) presented in Fig. 4.

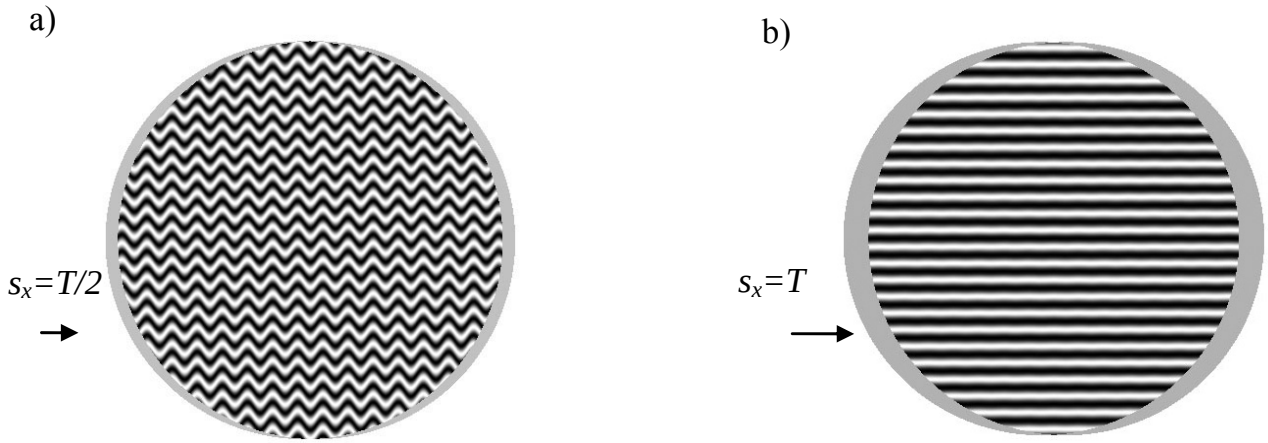

Fig.5. Lateral shear interferograms of test object $\varphi(x,y) = \sin\left[2\pi\left(\frac{x}{D/20}\right)\right]$, for two shear values of a) s = (D/40); b) s = (D/20).

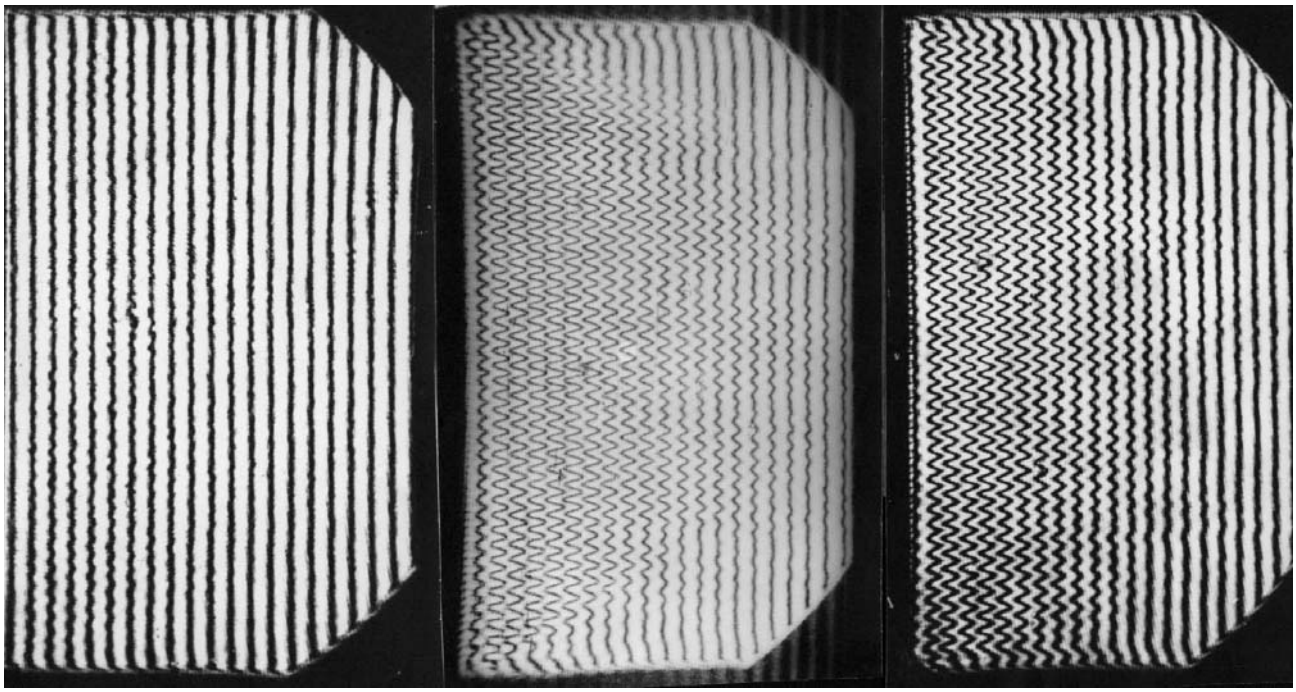

a) b) c)

Fig.6. Nozzle grid shear interferograms

Fig.6 shows two-dimensional flow interferograms after a "flat" constant step nozzle grid.

GAS FLOW SHEAR INTERFEROGRAMS AND SHADOW PATTERNS INFORMATIVITY COMPARATIVE ANALYSIS

Lateral shear interferometer sensitivity is a function with a period of 1/s as shows expressions (2) and Fig. 4. Wave function distortion amplitude information on the shear interferogram is completely absent at frequencies $\nu = n/s, \quad n = 0,1,...$ however double sensitivity compared to the same object reference wavefront interferogram takes place on frequencies $\nu = (n + 0,5)/s, \quad n = 0,1,...$. For example, Fig. 5. shows calculated shear interferogram models: in Fig. 5a shear is half of the harmonic distortion period, : in Fig. 5b shear is equal to the harmonic distortion period.

On the interferogram a) shear is equal to nozzle array step; b) – shear is half of the harmonic nozzle array step, i.e. condition $\nu \cdot s = 0,5$ is satisfied; c) – shear value is intermediate $0 < \nu \cdot s < 0,5$

Testing object joint two interferogram processing with a nonmultiple collinear lateral shear values allows avoiding information loss at a shear multiple spatial frequencies [5, 6].Another second type information loss compensation option is possible for specific gas-dynamic medium like the study of isotropic turbulence spectrum gas-dynamic medium, for example, using radial and reverse shear interferometers.

Wavefront spectrum can be represented as a spectra linear combination obtained by two shear interferogram processing in case of nonmultiple shear value two interferogram registration. Thus joint spatial spectral informativity of the two interferograms H1(ν) и H2(ν) can be expressed as:

$$\Phi(\nu) = \frac{H_1(\nu) \cdot \left|1 - \exp(-i2\pi s_1 \nu)\right| + H_2(\nu) \cdot \left|1 - \exp(-i2\pi s_2 \nu)\right|}{\left|1 - \exp(-i2\pi s_1 \nu)\right| + \left|1 - \exp(-i2\pi s_2 \nu)\right|} \qquad (3)$$

Second type information loss could be almost completely eliminated with proper, shear s1 и s2 selection. As an example, Fig.7 shows spectral "sensitivity" interference system graph (proportional to the weight function), obtained with two shear values s and 1.093s.

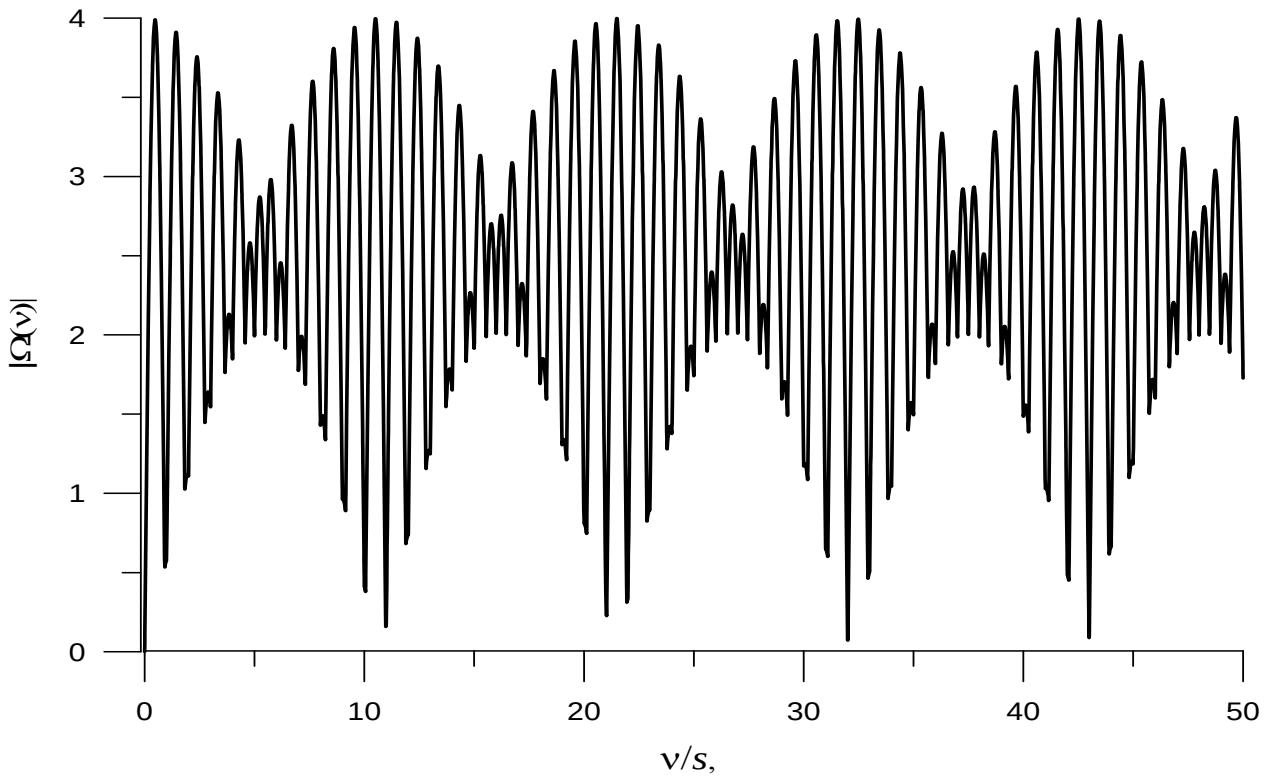

Fig.7. lateral shear interferometer spectral spatial "sensitivity" graph for joint interferogram processing with the shear value of s and 1.093s.

Spatial frequencies bandwidth may have a complex shape for shadow instruments as well as shear interferometers. signal frequency spectrum is explicitly regulated by the knife-edge position for considering scheme variant, Fig. 1. Any knife-edge displacement causes corresponding harmonics complete loss due to knife-edge screening or the phase contrast loss due to positive and negative signal frequencies passing. Shadow patterns corresponding to the knife displacement in the Fourier plane shown in Fig. 8.

Shadow pattern contrast becomes nearly zero at the knife offset value more than instrument Fourier plane $\delta = \frac{\lambda f}{(D/20)}$ linear harmonic coordinates as shown on Fig. 8.

Such a dependence on the knife-edge setting accuracy may adversely affect the measurements quality since the optical wedge appearance in the flow (that is common) causes test beam translational amplitude distribution displacement in the Fourier plane and, consequently, information loss about the number of flow phase distortion frequency components.

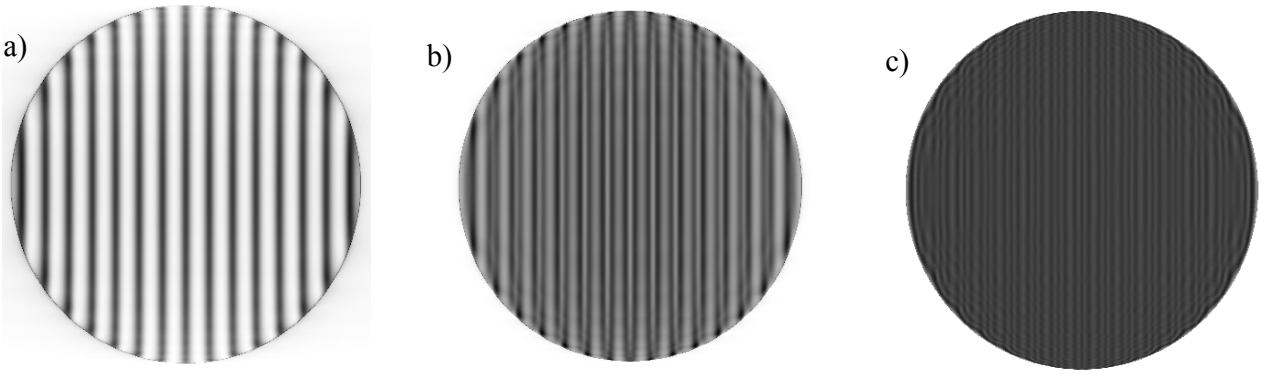

Fig.8. Shadow patterns, obtained with harmonic wavefront distortion $\varphi(x,y) = \sin\left[2\pi\left(\frac{x}{D/20}\right)\right]$ for knife edge offset equal to a) Δ=0; b) $\Delta = 0.6\frac{\lambda f}{(D/20)}$; c) $\Delta = 1.2\frac{\lambda f}{(D/20)}$.

INCOMPLETE OBJECT IMAGE FILLING. The third information loss type caused by incomplete filling investigated object image by interference pattern characteristic only for the shear interferometers. For the spatially restricted beams expression (1) takes the form:

$$\Psi'(\nu) = \Phi'(\nu)\cdot\left[1-\exp(-i2\pi s\nu)\right] + L(\nu), \quad (4)$$

where:

$$\Psi'(\nu) = \cdot F[\psi'(x)]; \qquad \Phi'(\nu) = F[\varphi'(x)];$$

$$\psi'(x) = \begin{cases} \psi(x) & x \in [s,D] \\ 0 & \text{all other cases} \end{cases}$$

$$\varphi'(x) = \begin{cases} \psi(x) & x \in [0,D] \\ 0 & \text{all other cases} \end{cases}$$

$$L(\nu) = -\int_0^s \varphi(x)\cdot\exp[-i2\pi\nu x]dx + \exp[-i2\pi\nu s]\int_{D-s}^{D}\varphi(x)\cdot\exp[-i2\pi\nu x]dx$$

where D – beam aperture.

Unlike the "infinite" aperture case function $\varphi'(x)$ has nonzero values only in the beam aperture area [0, D], and function $\psi'(x)$ - in the interference field of sheared relative to each other beams, i.e. recorded investigated object image [0, s] part does not contain the interference pattern.

Expression (4) can be used to reconstruct the lateral shear interferograms wave front, if function L(ν) is known. As shown in [4] this function can be determined if there is a priori wave front behavior information on any beam aperture interval length equal to the shear vector value s. The absence of this information leads to the wavefront information distortions discrecity with a step equal to the shear value, i.e. unambiguous wavefront restoration is possible in a discrete points set with a spatial step equal to the shear s.

In contrast to the optical shop testing tasks mentioned part of the object in the segment [0, s] usually contains an interference pattern in the flow study. Gas-dynamic medium under study density distribution can be reconstructed on the interferogram without the third information loss type disadvantages if this image element is undisturbed flow part.

GAS FLOW SHEAR INTERFEROGRAMS AND SHADOW PATTERNS INFORMATIVITY COMPARATIVE ANALYSIS

SYSTEMS COMPARISON. Important measuring system characteristics are the precision and measurement dynamic range besides instrument sensitivity anisotropy and transfer function. According to these parameters interferometric systems have a significant advantage over the shadow instruments.

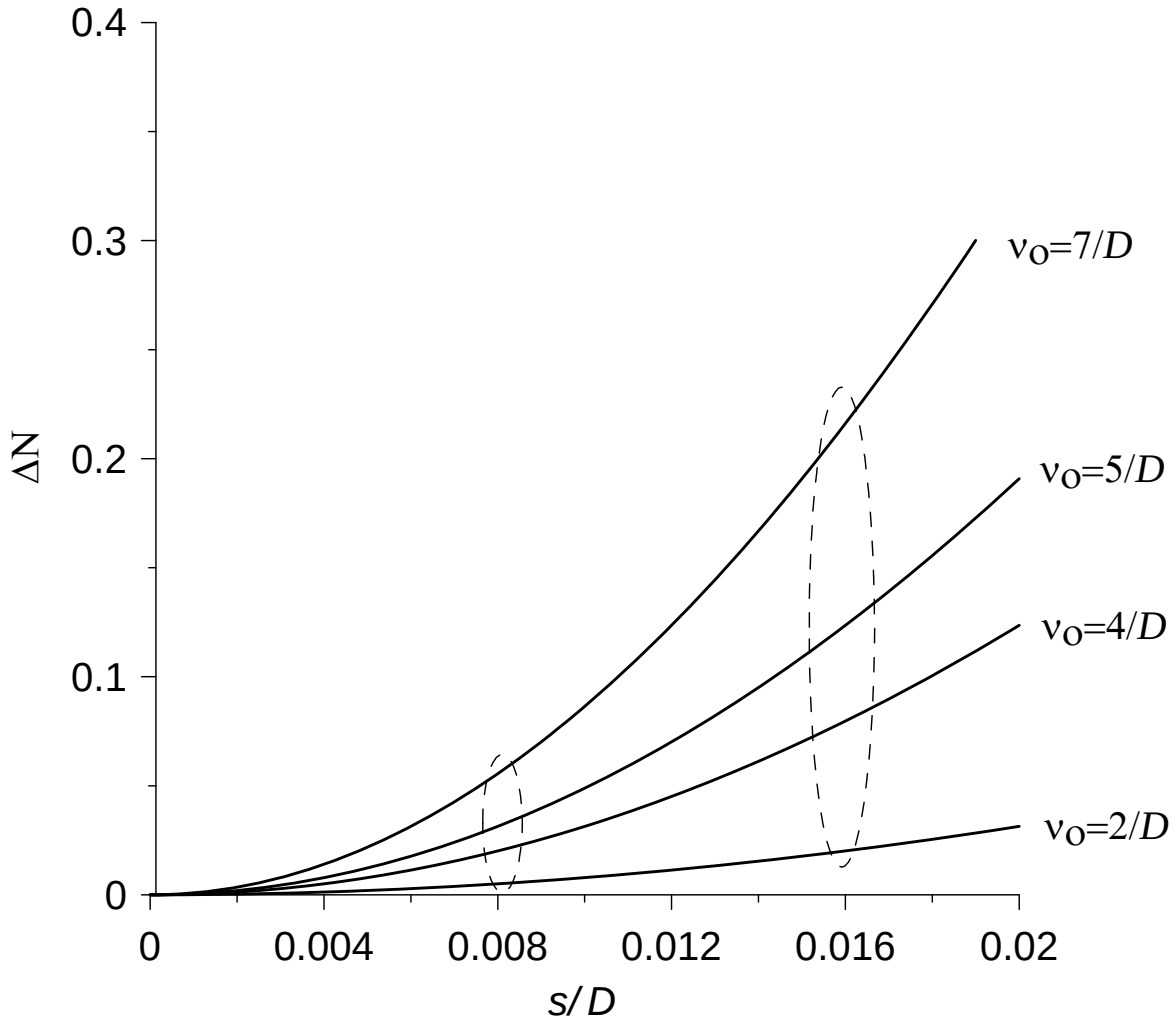

Fig.9. Interference fringe displacement dependency for different spatial frequencies νo harmonic phase distortion from relative shear value.

Fig. 9 presents interference bands displacement dependence (expressed as a bandwidth fraction) of the shear value for different harmonic frequency phase perturbations. As you can see, the transition from the shear s/D = 1.6% to s/D = 0.8% average interferometer sensitivity falls almost four times.

This feature allows adjusting the shear interferometers for the a priori known gas flow characteristics. In principle, this allows (which appears in the interference fringes gap particularly in reference wavefront interferometers) to obtain quantitative information even with the supersonic flows shock without loss of information [7]. Can be seen in Fig. 10 flow regions, separated by such shock. However, the shear value selection has yielded quantitative areas density relation of shock-divided flow.

The shadow instruments quantitative measurements dynamic range is noticeably inferior to shear systems. Fig. 11 shows comparison testing beam calculated image intensity distribution obtained for the two measuring systems by varying the phase harmonic distortion amplitude.

Shadow patterns quantitative processing error exceeds such of shear interferograms due to the detected signal parameters difference. In shadow pattern processing each detector pixel records the total intensity determined by adding the testing different aperture part light beams where gas dynamics medium is observed. In the shear pattern fringe displacement characterizes the phase difference between similar aperture sections. Moreover specified shear interferogram property reduces the demands to the detecting camera linearity and to the amplitude noise presence on the interference pattern.

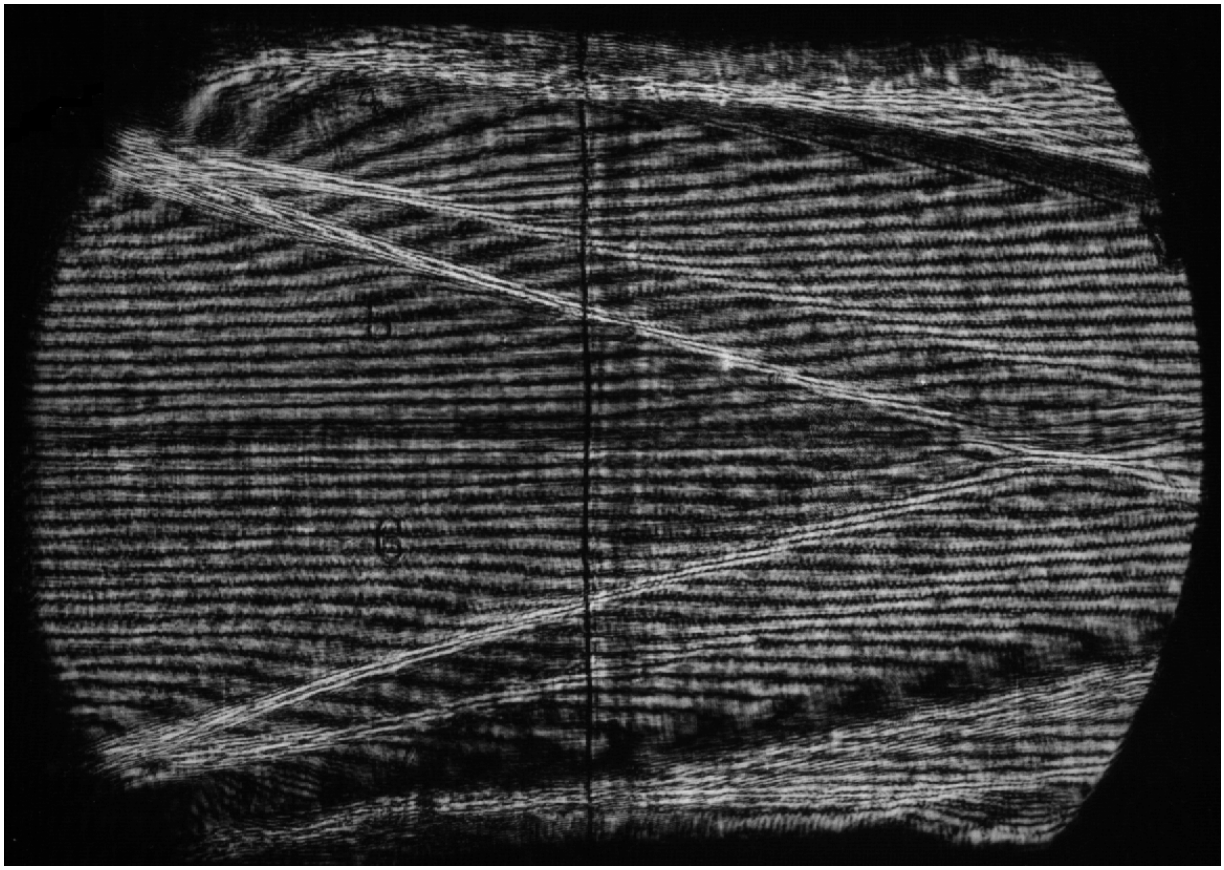

Fig.10.

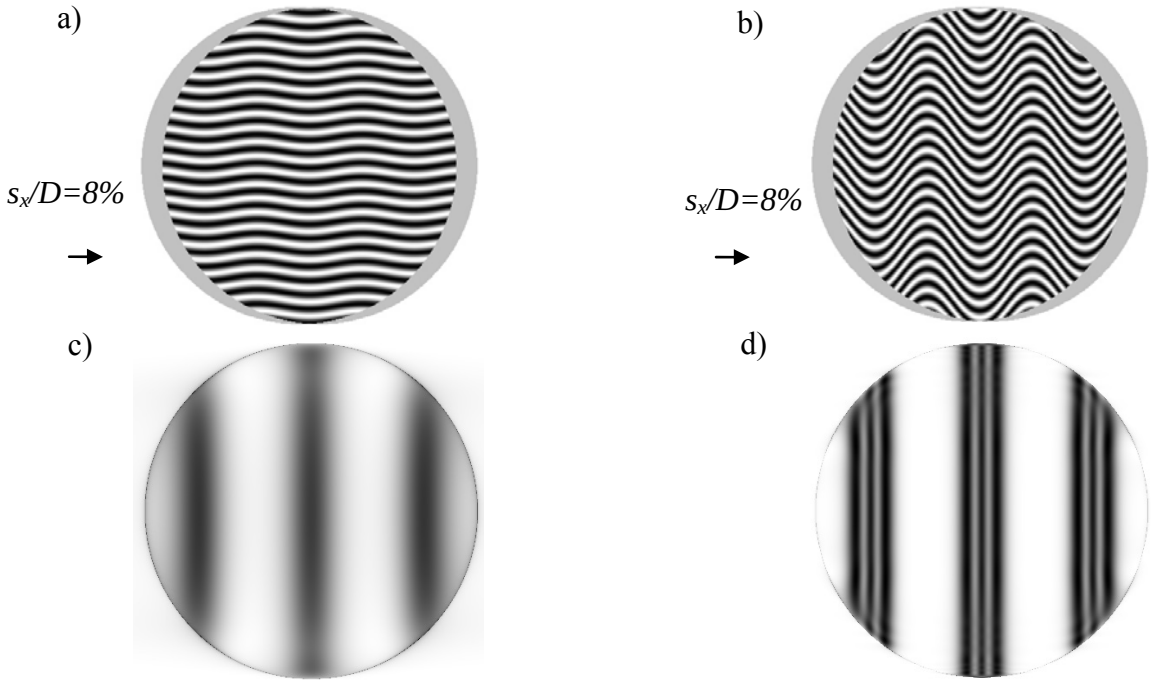

Fig.11. Shear (a,b) and shadow (c,d) calculated patterns obtained by testing the harmonic phase inhomogeneities $\varphi(x,y)=\phi\sin\left[2\pi\left(\frac{x}{D/4}\right)\right]$ where ϕ = 1 (a,c) and ϕ = 8 (b,d).

GAS FLOW SHEAR INTERFEROGRAMS AND SHADOW PATTERNS INFORMATIVITY COMPARATIVE ANALYSIS

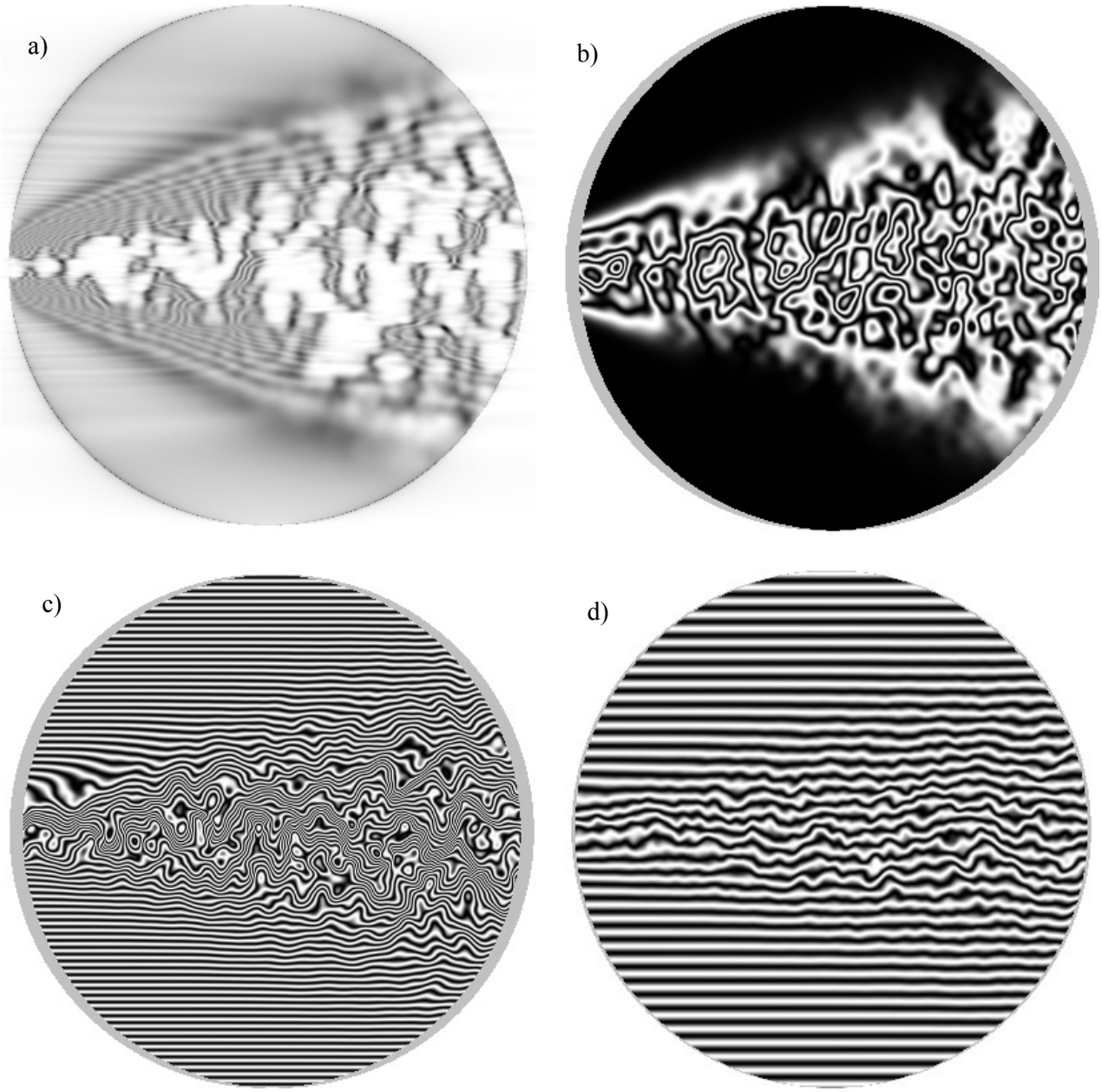

Fig.12. Shadow (a) and shear (b,c,d) calculated gas flow model patterns

Fig. 12 illustrates differences between shadow and shear interference patterns in resolution of refractive index random distribution structure details in a gasdynamic medium.
Shear interference and shadow patterns are used mainly for gas flows visualization at low shear values and highest possible fringe width. Fig. 12 shows the numerical simulation result of turbulent gas flow with shadow instrument (fig. 12a) and shear interferometer with "infinitely" wide interference fringe (fig. 12b). Finite fringe mode (fig. 12c) allows obtaining specific information about the density distribution in some flow sections.
Adjusting shearing interferometer dynamic range allows to fully getting a gas-dynamic medium density distribution quantitative results by setting testing object image shear (fig. 12d).

CONCLUSION. Features and advantages of the of shear interferometry method in comparison with other gas dynamic medium visualization based optical methods are following:
1- Dynamic processes visualization ability often exceeds the shadow methods resolution, and not inferior to the reference wave front interferometry;
2- Shearing interferometer systems allows adjusting the sensitivity and dynamic range of the measured parameters in contrast to those mentioned above in paragraph 1;
3- Shearing interferometer systems are the most technically realizable in the bench and field studies;
4- The possibility to obtain studied gas dynamic medium quantitative characteristics exceeds mentioned above in paragraph 1 systems;

5- Shear interferometry systems hardware based on components with minimal technical characteristics requirements, for example, recording camera linearity, image noise presence, illumination inhomogeneity, optical components quality, etc.

Refences

1. Soroko L.M. // Gilbert Optics, Moscow, "Nauka", (1981).
2. Skotnikov M.M. // Shadow quantitative methods in gas dynamics, Moscow, "Nauka", (1976).
3. V.N.Shekhtman. // Construction of light wave front from lateral shearing interferograms, Sov.J.Opt. Technology, 49, (10), Oct. (1982).
4. V.N.Shekhtman. A.Yu.Rodionov, A.G.Pel'menev, // Reconstruction of a Light Beam Wave Front by Synthesis of a Shear Interferogram, Optics and Spectroscopy, vol.76, No 6, pp.884-888, (1994)/
5. V.N.Shekhtman, A.Yu.Rodionov, A.G.Pel'menev. // Full Reconstruction of a Light Beam Wave Front from a Synthesized Shear Interferogram, vol.79, No 1, pp.124-127, (1995)/
6. V.N.Shekhtman. Synthesis of interferograms by lateral shear to measure wave front of a light beam, Proceeding of the NATO Advanced Research Workshop on Optical Resonators – Theory and Design, Smolenice Castle, Slovak Republic, July 1-5, 1997. Series: Nato Science Partnership Subseries: 3, Vol. 45, Editor » Kossowsky, R. (at al), Kluwer Academic Publishers, Dordrecht/Boston/London, pp. 301-307, (1998).
7. S.I. Inshakov, A.Yu. Rodionov, A.S. Shirin, V.N. Shekhtman. Interferometer for simultaneous registration two ortogonical directional lateral shear interferograms, *OPTICAL METHODS OF FLOW INVESTIGATION.* Proc. of the 11th International Scientific and Technical Conference OMFI-2011, Moscow, Russia, (2011).